High-order curvatures and harmonicity regression

1997 J. Phys. A: Math. Gen. 30 7009

(http://iopscience.iop.org/0305-4470/30/20/008)

J. Phys. A: Math. Gen. **30** (1997) 7009–7020. Printed in the UK PII: S0305-4470(97)81176-6

High-order curvatures and harmonicity regression

Carlo Alabiso† and Mario Casartelli‡

Dipartimento di Fisica dell'Università di Parma, 43100 Parma, Italy

Received 21 January 1997, in final form 7 April 1997

Abstract. We consider curvatures κ_i of all orders, as defined by the generalized Frenet–Serret formulae, along the trajectories of a classical Hamiltonian system with N degrees of freedom. In the spirit of previous experiments on the first two of them, time averages are numerically computed for the curvatures up to fifth order and for the microcanonical density in a typical anharmonic system (the FPU quartic chain), with checks in other models. Neat breakdowns of harmonic-like behaviour define thresholds to anharmonicity for every κ_i at distinct values $\tilde{u}_i$ of the order parameter (the energy density u). The threshold $\tilde{u}_i$ at fixed order i is independent of the total N, and it rapidly decreases as i grows. However, all curvatures are simultaneously sensitive or not to the initial conditions, for $u < \tilde{u}_1$ or $u > \tilde{u}_1$ respectively, confirming the previous identification of $\tilde{u}_1$ as an efficient indicator of the strong stochasticity transition. This phenomenology, which is discussed within the weak/strong stochasticity problem, gives a new insight into the progressive enforcement of a harmonic-like structure as u decreases.

1. Introduction

In [1], indicators of the deviations from a harmonic-like behaviour of Hamiltonian models (Fermi–Pasta–Ulam (FPU), Lennard–Jones (LJ), Toda, etc) have been introduced. They are based on the Frenet–Serret curvature κ and torsion τ of trajectories in the phase space, and on the microcanonical density ρ. The formers have a clear geometrical character, related to the shape of the trajectory; the latter admits both geometrical and dynamical interpretations, since it may be associated to the steepness of the energy surface and to the phase velocity. The microcanonical density is indeed given by the inverse modulus of the gradient of the energy surface and, equivalently, by the the sojourn time of the phase point along the trajectory on the same surface.

It has been found that these anharmonicity indicators undergo a drastic change (harmonicity breakdown) in a certain range of values of the order parameter, the specific energy u. Moreover, for the non-integrable systems, below or above this range the indicators result to be sensitive or not, respectively, to the initial conditions. Actually, the discussed range coincides with the so-called strong stochasticity threshold (SST) elsewhere established by equipartition-based methods or Lyapunov exponents, thus proving the new method to be an alternative approach to the SST. In this context, its peculiarity with respect to standard methods consists of the fast and precise localization of the breakdown range, leaving only a few long experiments for the necessary checks on initial conditions sensitivity. Some references relevant for this discussion are [2–11].

† INFN Gruppo collegato di Parma. E-mail address: alabiso@pr.infn.it

‡ INFM, Parma. E-mail address: casartelli@pr.infn.it

0305-4470/97/207009+12$19.50

Other geometrical approaches to the study of stochasticity have been proposed, and we refer in particular to those based on the Ricci and scalar curvatures in the configurations space [12–14]. Basically, they use intrinsic (i.e. independent of coordinates) observables, giving evidence to possible sources of stochasticity, such as abundance of subdomains with negative (Ricci) curvature and parametric resonance. A 'weak chaos' assumption is made there when, for instance, the authors compare dynamical to Monte Carlo simulations even *below* the SST. This approach, apart from the neatness of the numerical indications, offers the advantage of important connections to other methods and concepts (e.g. Lyapunov exponents).

The geometrical character of the analysis developed in [1] is to be intended differently: actually, coordinate-dependent observables have been chosen to give evidence to the *possible* stable vicinity to equivalent harmonic trajectories. This means to explore the *practical* persistence of a toroidal structure in the phase space, by observing the consequences of such 'effective' surfaces on the observables. In doing this, no assumption has been made about the existence of weak chaos, whose possible relevance for statistics in our opinion is still to be understood.

Anyway, the main question in [1] was the very existence of a stochasticity transition. For this reason, an experimental fact was remarked there but not further studied: by looking more closely at the range of transition values for u, while the behaviour of ρ and κ looked very similar to each other, there was a systematic ordering of the transition values obtained via κ or τ. Precisely, the second one was always smaller.

Our intention here is to understand the true significance and implications of such a fine structure, by considering, as a starting point, the natural extension of the previous observables: as it is well known, for a curve in $\mathbf{R}^n$ there are $n-1$ curvatures $\{\kappa_i\}$, the standard curvature and torsion being the first two of them ($\kappa \equiv \kappa_1, \tau \equiv \kappa_2$). By this sequence of observables a rich structure in the non-stochastic region of the phase space appears, in the form of a sequence of harmonicity thresholds $\tilde{u}_1, \tilde{u}_2, \tilde{u}_3, \ldots$, one for each observable $\kappa_1, \kappa_2, \kappa_3, \ldots$. This means that the consolidation of harmonicity takes place progressively through a sequence of steps. Even if not a true discontinuity, this introduces a discretized degree of harmonicity—and, consequently, of order—directly measured on the trajectories. An interesting point is that this structure is independent of N, also quantitatively.

We observe that while stochasticity implies the destruction of harmonic trajectories, the progressive vanishing of harmonicity in itself does not imply stochasticity, as the Toda counterexample shows. But, in contrast, the persistence of harmonicity is a strong indication against a genuine stochasticity. In other words, harmonicity is a sufficient but non-necessary criterion of non-stochasticity, and the higher and higher degree of harmonicity corroborates the idea of growing difficulties for an erratic behaviour. Also the independence of N is coherent with this perspective. In this sense, even if the persistence of a harmonic structure does not exclude, in principle, the existence of Arnol'd diffusion, topological transitivity and, consequently, weak chaos, our experiments support the possibility that the SST is the only transition relevant for statistical mechanics.

In conclusion, the method developed here not only emphasizes the previous results—coincidence of SST and κ_1 harmonicity breakdown—but proves able, in addition, to characterize the degree of order, and implicitly what weak chaos could mean. The onset of order exhibits a structure much more complicated than the simple connection to the $\tilde{u}_1$ threshold. The method is a non-perturbative one, since it does not directly care about the existence or destruction or deformed KAM tori when a certain order parameter is modified. Thus, with respect to the delicate task of following perturbatively the persistence of quasi-

integrability, this approach offers the advantage of treating directly the consequences entailed by the dynamics on the observables. Moreover, it is mathematically simple.

2. Frenet–Serret equations, models and observables

In the Euclidean space $\mathbf{R}^n$ of coordinates $x_1, x_2, \ldots, x_n$, consider a curve $\Gamma(s)$ as a function of the curvilinear coordinate

$$s = \int_0^{\{\bar{x}_i\}} \mathrm{d}s = \int_0^{\{\bar{x}_i\}} \sqrt{\mathrm{d}x_1^2 + \mathrm{d}x_2^2 + \ldots + \mathrm{d}x_n^2}. \tag{1}$$

If the curve is C^n in s with n linearly independent derivatives, it locally defines a complete orthonormal system of vectors, iteratively obtained by the equations:

$$\kappa_i \boldsymbol{v}_{i+1} = \frac{\mathrm{d}\boldsymbol{v}_i}{\mathrm{d}s} + \kappa_{i-1}\boldsymbol{v}_{i-1} \qquad i = 1, \ldots, n-1 \tag{2}$$

with:

$$|\boldsymbol{v}_1| = |\boldsymbol{v}_2| = \ldots = |\boldsymbol{v}_n| = 1 \qquad \kappa_0 \boldsymbol{v}_0 = 0 \qquad \boldsymbol{v}_1 = \frac{\mathrm{d}\Gamma}{\mathrm{d}s}. \tag{3}$$

(See for example [15].) This is equivalent to defining the versors $\boldsymbol{v}_i$ by the usual Gram–Schmidt orthonormalization of the derivatives. For $n = 3$ equations (2) are the standard Frenet–Serret relations, with $\boldsymbol{v}_1 = \boldsymbol{t}, \boldsymbol{v}_2 = \boldsymbol{n}, \boldsymbol{v}_3 = \boldsymbol{b}, \kappa_1 = k, \kappa_2 = \tau$; the vectors $\boldsymbol{t}, \boldsymbol{n}, \boldsymbol{b}$ are the tangent, normal and binormal versors, and k, τ the usual curvature and torsion. The curvature measures the variation of the tangent versor, whereas the torsion measures the variation of the osculating plane Π_2.

In the general case, the ith curvature κ_i measures the istantaneous variation along the motion of the i-dimensional manifold Π_i, defined by the versors $\{\boldsymbol{v}_1, \boldsymbol{v}_2, \ldots, \boldsymbol{v}_i\}$ *outside* Π_i itself. From equation (2), it follows that the first $i-1$ versors $\boldsymbol{v}_1, \boldsymbol{v}_2, \ldots, \boldsymbol{v}_{i-1}$ move inside the manifold, and only $\boldsymbol{v}_i$ gains the contribution $\kappa_i \boldsymbol{v}_{i+1}$ outside of Π_i. Alternatively, the variation of the manifold Π_i can also be seen through the variation of its normal, as obtained by looking at two consecutive FS formulae projected on the plane $\{\boldsymbol{v}_i, \boldsymbol{v}_{i+1}\}$:

$$\begin{cases} \left(\dfrac{\mathrm{d}}{\mathrm{d}s}\boldsymbol{v}_i\right)\Big|_{\{i,i+1\}} = \kappa_i \boldsymbol{v}_{i+1} \\ \left(\dfrac{\mathrm{d}}{\mathrm{d}s}\boldsymbol{v}_{i+1}\right)\Big|_{\{i,i+1\}} = -\kappa_i \boldsymbol{v}_i. \end{cases} \tag{4}$$

These equations reflect the equality of the triangles defined by the versors $\boldsymbol{v}_i$ and $\boldsymbol{v}_{i+1}$ and by their infinitesimal variations on the plane during the motion.

Actually, we are interested in curves that are solutions of Hamiltonian systems. Since this paper is an extension of [1], we refer to it for details on this point. For reading convenience we only recall some definitions, related to one-dimensional chains of N particles with unitary mass, whose trajectories develop in a $2N$-dimensional phase space.

The harmonic Lagrangian is:

$$\mathcal{L}_0(\boldsymbol{x}) = K - \chi V_2 = \frac{1}{2}\sum_{j=1}^{N} \dot{x}_j^2 - \frac{\chi}{2}\sum_{j=1}^{N}(x_j - x_{j+1})^2. \tag{5}$$

The FPU system has the anharmonic potential:

$$\varepsilon V_4(\boldsymbol{x}) = \frac{\varepsilon}{4}\sum_{j=1}^{N}(x_j - x_{j+1})^4 \qquad (x_1 = x_{N+1}). \tag{6}$$

The LJ and Toda systems are described by the potentials:

$$V_{LJ} = 4\hat{\varepsilon}\sum_{j=0}^{N}\left[\left(\frac{\sigma}{x_j - x_{j+1} + x_{eq}}\right)^{12} - \left(\frac{\sigma}{x_j - x_{j+1} + x_{eq}}\right)^{6}\right] + (N+1)\varepsilon \qquad (x_0 = x_{N+1} = 0) \tag{7}$$

and

$$V_T = \alpha\sum_{j=0}^{N}(\mathrm{e}^{-\beta(x_j - x_{j+1})} + \gamma(x_j - x_{j+1})) \qquad (x_0 = x_{N+1} = 0) \tag{8}$$

respectively. Note that V_{LJ} and V_T include also the harmonic potential of the Lagrangian (5). Actually, the boundary conditions have been proven to be non-relevant for the properties we are dealing with.

In the canonical homogeneous coordinates $(\boldsymbol{p}, \boldsymbol{q})$, the harmonic Hamiltonian reads:

$$H_0(\boldsymbol{p}, \boldsymbol{q}) = \frac{1}{2}\sum_{k=1}^{N}\omega_k(p_k^2 + q_k^2) = \sum_{k=1}^{N}E_k \tag{9}$$

where E_k denotes the energy of the kth harmonic mode. The frequencies with periodic boundary conditions are twofold degenerate, and are given by:

$$\omega_k = 2\sqrt{\chi}\sin\frac{((k-1)\pi)}{N} \tag{10}$$

while those with fixed boundary conditions are non-degenerate, and read:

$$\omega_k = 2\sqrt{\chi}\sin\frac{k\pi}{2(N+1)}. \tag{11}$$

With homogeneous canonical coordinates $(\boldsymbol{p}, \boldsymbol{q})$ the differential of the curvilinear coordinate along a trajectory in the phase space is:

$$\mathrm{d}s = \left(\sum_{k=1}^{N}(\mathrm{d}p_k^2 + \mathrm{d}q_k^2)\right)^{\frac{1}{2}} \tag{12}$$

the tangent versor is given by

$$\boldsymbol{t} = \boldsymbol{v}_1 = \{\mathrm{d}p_1/\mathrm{d}s, \ldots, \mathrm{d}p_N/\mathrm{d}s, \mathrm{d}q_1/\mathrm{d}s, \ldots, \mathrm{d}q_N/\mathrm{d}s\} \tag{13}$$

and the other quantities follow directly from FS equations. We have made experiments (with increasing numerical difficulties) on the first five curvatures. Further, we considered the inverse of the velocity along the trajectory, i.e. the microcanonical density:

$$\rho = \frac{1}{|\nabla H(\boldsymbol{p}, \boldsymbol{q})|} = \left|\frac{\mathrm{d}\Gamma}{\mathrm{d}t}\right|^{-1} = \frac{\mathrm{d}t}{\mathrm{d}s} = |\boldsymbol{v}|^{-1} \tag{14}$$

where $\boldsymbol{v}$ denotes the phase space velocity.

In the harmonic limit, higher curvatures can be obtained by induction from the explicit expressions of the first vectors:

$$\begin{aligned} &\boldsymbol{v}_1|_k = \rho\omega_k(-q_k, p_k) \qquad \kappa_1\boldsymbol{v}_2|_k = (\rho\omega_k)^2(-p_k, -q_k) \\ &\kappa_2\boldsymbol{v}_3|_k = ((\rho\omega_k)^3/k_1 - \kappa_1\rho\omega_k)(q_k, -p_k). \end{aligned} \tag{15}$$

In fact, all the vectors have the same structure:

$$\kappa_i\boldsymbol{v}_{i+1}|_k = \xi_i^k W_{ik} \tag{16}$$

with

$$\begin{aligned} W_{1k} &= (-p_k, -q_k) \qquad W_{2k} = (q_k, -p_k) \\ W_{3k} &= (p_k, q_k) \qquad W_{4k} = (-q_k, p_k) \end{aligned} \tag{17}$$

and further on with periodicity of 4, and with the functions ξ_i^k satisfying the recurrence relation:

$$\xi_i^k = \frac{\rho\omega_k}{\kappa_{i-1}}\xi_{i-1}^k - \frac{\kappa_{i-1}}{\kappa_{i-2}}\xi_{i-2}^k. \tag{18}$$

From (16) and (17) it follows:

$$|\kappa_i|^2 = \sum_{k=1}^{N} |\xi_i^k|^2 (p_k^2 + q_k^2). \tag{19}$$

The above equations state that all the harmonic curvatures are dimensionally homogeneous to $\rho\omega_k$, and moreover that they have the same dependence on the energy as ρ has.

We give the explicit formulae of microcanonical density and curvatures up to order five:

$$\begin{aligned} \rho &= \left[2\sum_k \omega_k E_k\right]^{-\frac{1}{2}} \\ |\kappa_1| &= \rho\left[2\sum_k \omega_k (\omega_k\rho)^2 E_k\right]^{\frac{1}{2}} \\ |\kappa_2| &= \rho\left[2\sum_k \omega_k \left(\frac{1}{\kappa_1}\left[(\omega_k\rho)^2 - \kappa_1^2\right]\right)^2 E_k\right]^{\frac{1}{2}} \\ |\kappa_3| &= \rho\left[2\sum_k \omega_k \left(\frac{1}{\kappa_2\kappa_1}\left[(\omega_k\rho)^3 - (\kappa_2^2 + \kappa_1^2)\omega_k\rho\right]\right)^2 E_k\right]^{\frac{1}{2}} \\ |\kappa_4| &= \rho\left[2\sum_k \omega_k \left(\frac{1}{\kappa_3\kappa_2\kappa_1}\left[(\omega_k\rho)^4 - (\kappa_3^2 + \kappa_2^2 + \kappa_1^2)(\omega_k\rho)^2 + \kappa_3^2\kappa_1^2\right]\right)^2 E_k\right]^{\frac{1}{2}} \\ |\kappa_5| &= \rho\left[2\sum_k \omega_k \left(\frac{1}{\kappa_4\kappa_3\kappa_2\kappa_1}\left[(\omega_k\rho)^5 - (\kappa_4^2 + \kappa_3^2 + \kappa_2^2 + \kappa_1^2)(\omega_k\rho)^3\right.\right.\right. \\ &\qquad \left.\left.\left. + (\kappa_4^2\kappa_2^2 + \kappa_4^2\kappa_1^2 + \kappa_3^2\kappa_1^2)\omega_k\rho\right]\right)^2 E_k\right]^{\frac{1}{2}}. \end{aligned} \tag{20}$$

From a direct inspection of (20) one can check that, as expected, the microcanonical density and all the harmonic curvatures behave as $E^{-1/2}$ or $u^{-1/2}$, for a linear rescaling of the harmonic energies E_k. By taking this behaviour into account in the harmonic limit, we can normalize the observables by defining

$$\kappa_i^{(n)} = \kappa_i/\rho \qquad \rho^{(n)} = \rho/E^{-\frac{1}{2}}. \tag{21}$$

These new observables are therefore constant in u in the harmonic system, depending on the initial conditions only through the ratios E_k/E. Therefore, *at all energies*, the initial conditions which keep such ratios fixed, provide the same harmonic reference values.

For the different normalizations of the κ_i and ρ there are two reasons: the first is empirical, as explained in [1], because the normalizations by ρ emphasize the deviations from harmonicity. The second reason is formal: taking into account $\rho = \mathrm{d}t/\mathrm{d}s$, we may write the FS formulae in the parameter t:

$$\frac{\mathrm{d}\boldsymbol{v}_i}{\mathrm{d}t} = \frac{\kappa_i}{\rho}\boldsymbol{v}_{i+1} - \frac{\kappa_{i-1}}{\rho}\boldsymbol{v}_{i-1} = \kappa_i^{(n)}\boldsymbol{v}_{i+1} - \kappa_{i-1}^{(n)}\boldsymbol{v}_{i-1} \tag{22}$$

where normalized curvatures only appear. The third of conditions (3) now reads:

$$\frac{\mathrm{d}\Gamma}{\mathrm{d}t} = \frac{1}{\rho}\boldsymbol{v}_1 \tag{23}$$

which provides the complete vector form of equation (14), further justifying our interest in the microcanonical density.

For each observables κ_i, ρ, $\kappa_i^{(n)}$, $\rho^{(n)}$, we evaluate time averages along the orbit, up to a time T that we choose big enough to stabilize the data:

$$\langle f \rangle = \frac{1}{T}\int_0^T f(\boldsymbol{p}(t), \boldsymbol{q}(t))\mathrm{d}t. \tag{24}$$

The normalization could be evaluated by the ratios of the averaged values, or by averaging the ratios. We have followed the first way for simplicity, after checking the practical irrelevance of the choice on the results.

3. Numerical experiments and results

As in [1], the simulations have been performed by using in (5)–(8) the following values of the parameters: $\chi = 1$, $\varepsilon = 0.1$, $\sigma = 1$, $\hat{\varepsilon} = 27.5$, $x_{eq} = 2^{\frac{1}{6}}\sigma$, $\beta = -2^{-1/6}$, $\gamma = \mathrm{e}\beta$ and $\alpha = 3.76$.

The number of degrees of freedom N ranges from 32 to 4096. We report the results referring to $N = 512$ only, since all the essential features are independent of N. For the FPU system, most of the experiments are performed on orbits corresponding to 800 of the shortest harmonic periods, and by averaging up to 5000 instantaneous values. Checks up to 8 times longer have been done for the averages, and even longer for the analysis of the dependence on the initial conditions. These times can be reduced for the Toda system, since, as expected, the stabilization is quite good even for short orbits. The specific energy u ranges from 3×10^{-5} to 30. The integration routine is a standard fifth order Runge–Kutta, and the integration steps have been chosen in order to ensure a good energy conservation (one part over 10^6, in the worst case). The Thinking Machine CM2 of the University of Parma was used.

All the experiments were performed with random initial conditions on the $\{\boldsymbol{p}\}$ and the $\{\boldsymbol{q}\}$ variables, sometimes with a further proportionality factor between them. By rescaling the variables we perform experiments at different energies E with fixed ratios E_k/E, and therefore with the same harmonic reference values of our normalized observables, as noticed after (21). We speak of a single class of initial conditions for different energies when they are obtained by the previous rescaling.

Figure 1, that also recovers some of the results obtained in [1], exhibits the final, well stabilized time averages of $\rho^{(n)}$ and $\kappa_i^{(n)} (i = 1, \ldots, 5)$ versus u, in the FPU system. The anharmonicity thresholds $\tilde{u}_i$ may be easily read. We obtain them through the crossover of two regimes: the first is the quasiharmonic one, the second is marked by a sudden increase of the anharmonicity up to a 'saturation' recognized in a flex point. The value $\tilde{u}_i$ is therefore the specific energy at the intersection between the harmonic straight line and the tangent in the flex. Evidently, such a value can be defined up to a certain approximation, and nevertheless the ordering $\tilde{u}_i > \tilde{u}_{i+1}$ is clearly established, as much as the coincidence (already noticed in [1]) of $\tilde{u}_1$ with the harmonicity breakdown for ρ, say $\tilde{u}_\rho$, and with the SST obtained through other methods. In the figure we report the results referring, for every u, to three classes of initial conditions, whose role is discussed below.

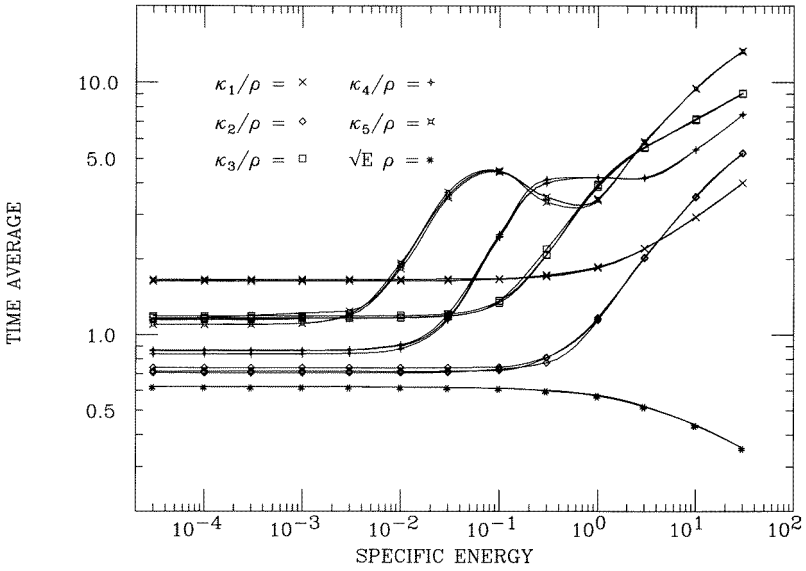

Figure 1. For three initial conditions, plots of time averaged and normalized $\kappa_1, \ldots, \kappa_5$ and ρ versus u, for the FPU model with $N = 512$. The total integration time corresponds to 800 of the shortest harmonic periods. The averages run over 5000 instantaneous values.

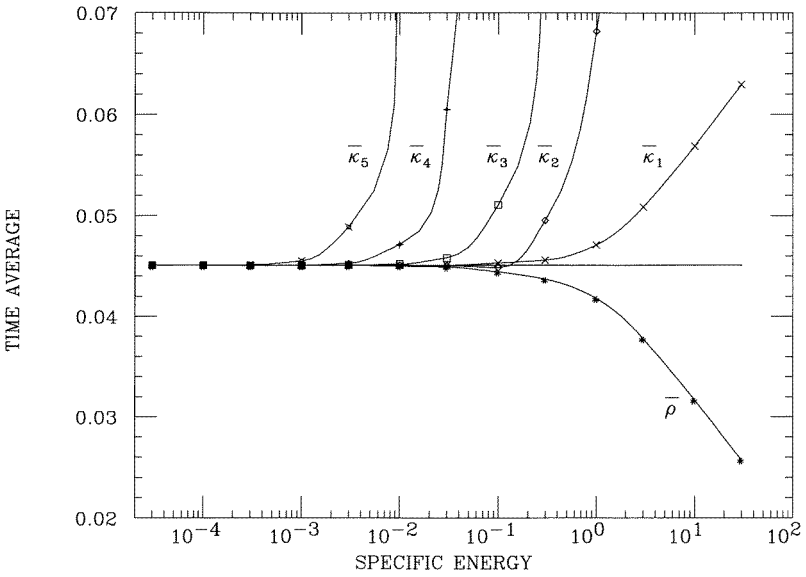

Figure 2. For a single initial condition, averaged and normalized $\kappa_1, \ldots, \kappa_5$ and ρ are plotted, after further normalization (indicated by the bar) to the harmonic limit of $\kappa_1\sqrt{u}$ (indicated by the straight line). Note the scale of the dependent variable, linear and nearly 300 times larger than in figure 1.

The evidence of the regression appears in figure 2, where, for a single class of initial conditions, we plot the same quantities of figure 1 after a further normalization that identifies the harmonic limits of $\kappa_2^{(n)}, \ldots, \kappa_5^{(n)}$ and $\rho^{(n)}$ with the harmonic limit of $\kappa_1\sqrt{u}$. Thanks to

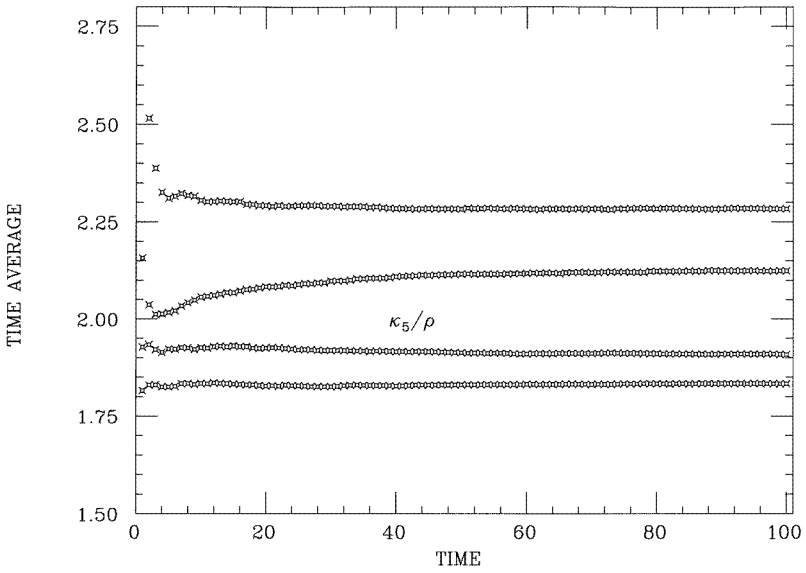

Figure 3. Time behaviour for averaged normalized κ_5 versus averaging time, for four initial conditions above its harmonicity breakdown ($u = 0.01$) but below breakdowns for $\kappa_1, \ldots, \kappa_4$ and ρ. The evolution length is 8 times longer than in figure 1.

the amplification of the observables over a linear and larger scale, beside the regression it is possible to appreciate a rough equispacing between the harmonicity breakdowns.

Supposing now that the relation $\tilde{u}_i > \tilde{u}_{i+1}$ might be extrapolated for all i, a question arises: Does the value $\tilde{u}_i$ mark a *stochasticity* threshold for the variable κ_i? In other words: What happens at a value u where some of the curvatures, say $\kappa_1, \ldots, \kappa_j$, are still quasiharmonic and the others, $\kappa_{j+1}, \kappa_{j+2}, \ldots$ have already lost the reference to the harmonic value? To answer this question, we checked the time behaviour of the averages over long orbits starting from several initial conditions at $u = 0.01$. Indeed, from figure 1, it results that κ_5 has already passed its breakdown value, whereas $\kappa_1, \ldots, \kappa_4$ did not. Figure 3 exhibits the time dependence of the averaged κ_5 over long orbits (8 times longer than the orbits used in figure 1) for four initial conditions: stabilization takes place over distinct final values. Equivalent results, of course, hold for the lower-order curvatures. This means that the harmonicity breakdowns do not imply any stochasticization, and that for $u < \tilde{u}_1$ the FPU system behaves as a non-ergodic one (see the Toda system below). Therefore, $\tilde{u}_1$ is qualitatively different from other thresholds. The onset of stochasticity at $u > \tilde{u}_1$ has been checked with the expected result: orbits starting from different initial conditions collapse into a unique final value. This appears in figure 4 for three initial conditions and the same total integration time as in figures 1 and 2.

Numerical experiments on the LJ chain present the same phenomenology, extending the results already obtained on the first two curvatures. Furthermore, in order to distinguish between harmonicity breakdowns and onset of stochasticity, experiments have been repeated on the integrable Toda chain. Figure 5 corresponds to figure 1 for this system: once again we observe a regression for the harmonicity breakdowns. In this case, however, $\tilde{u}_1$ does not have any peculiarity: there is a stable dependence on the initial conditions for all curvatures and energies. Therefore we do not report the time behaviours of observables, similar to those of figure 3, but even more regular.

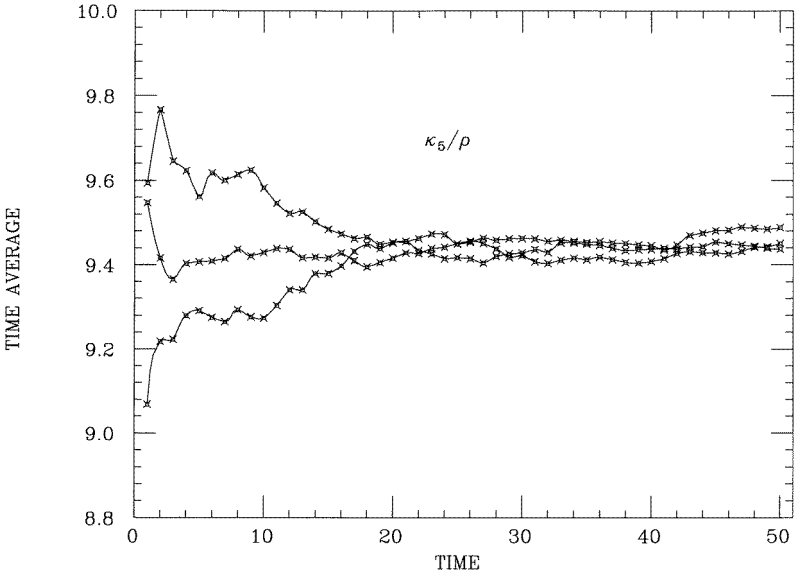

Figure 4. Time behaviour for averaged normalized κ_5 versus averaging time for three initial conditions, at energy above $\tilde{u}_1$ ($u = 10$) with parameters as in figure 1.

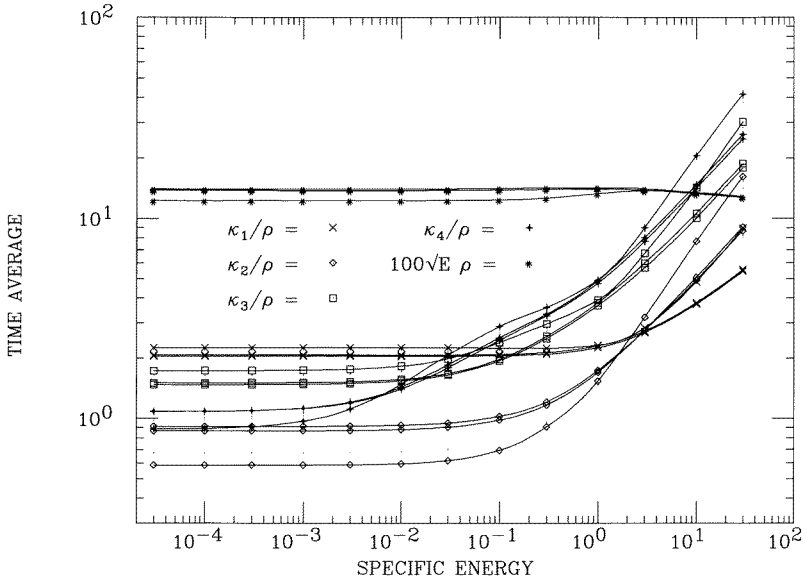

Figure 5. For three initial conditions, plots of time averaged and normalized $\kappa_1, \ldots, \kappa_4$ and ρ versus u for the Toda model with $N = 512$. The last curvature κ_5 is omitted because of instabilities in numerical simulations.

We recall that, as in [1], the parameters of the Toda model have been tuned up in order to make comparable the values of $\tilde{u}_1$ in this system and in the FPU system: the coincidence is therefore a matter of choice, not a result. (By choosing the parameters in such a way as to impose the coincidence of the harmonic limits, the value $\tilde{u}_1$ for Toda would be indeed

two orders of magnitude greater than the corresponding value for FPU.) In figure 5 it seems that curves corresponding to different initial conditions melt together around $\tilde{u}_1$, before separating again: but this is only an accident, and other initial conditions would not show this phenomenon.

For the FPU and the LJ systems, the regression of the harmonicity breakdowns $\tilde{u}_i$, as the order i of curvature κ_i grows, displays in conclusion the following features.

F1—At any order, the value $\tilde{u}_i$ depends on i but it is independent of the total N: there is therefore evidence that it could persist in the thermodynamic limit.

F2—The empirical relaxation time required to establish the value $\tilde{u}_i$ within a fixed precision, is roughly independent of the total N and also i.

F3—Looking at the time behaviours, above $\tilde{u}_1$ *all* the curvatures lose the memory of the initial conditions, while below $\tilde{u}_1$ all of them keep this memory.

F4—The transition values $\tilde{u}_i$ show a clear tendency to decrease. For $i = 1, \ldots, 5$ they appear roughly equispaced in the log scale, i.e. exponentially decreasing. We note that, by the iteration of FS equations, every κ_i contributes to all subsequent curvatures; therefore the harmonicity breakdown for κ_i implies that all higher curvatures are no more harmonic. This observation is sufficient to explain a weak ordering, i.e. $\tilde{u}_i \geqslant \tilde{u}_{i+1} \geqslant \cdots$, but it does not imply neither the strict ordering nor the exponential decreasing. The possible persistence of such an exponential rate for all $i > 5$ constitutes a plausible extrapolation, lacking, however, experimental evidence and theoretical explanation.

F5—Being finite, the sequence $\{\tilde{u}_i\}$ has a minimum: $\tilde{u} = \tilde{u}(N) \leqslant \tilde{u}_i$. Since the sequence is (at least) not increasing, the minimum $\tilde{u}(N)$ is the last one, but not necessarily $\tilde{u}_{2N-1}$ because, depending on the curve, the sequence of the κ_i could stop before the maximal order being attained. This happens, for instance, when a curve is confined in a subspace of the embedding space.

The meaning of this minimum is that for $u < \tilde{u}$ every curvature is quasiharmonic. A reasonable possibility is that, for $N \to \infty$, $\tilde{u}(N) \to 0$. However, since the sequence is very rapidly decreasing, for all practical purposes we may assume $\tilde{u}(N) \approx 0$ already for N in the range of our experiments. It is important to note that the alternative possibility, i.e. the existence of a *finite* limit for $\tilde{u}(N)$ as $N \to \infty$, would only enforce the conclusions we shall draw in the next section. In other words, the assumption of making $\tilde{u}$ vanish is the most severe one with respect to our arguments.

4. Final remarks

To summarize, we have discovered a discretized degree of harmonicity, leading to a criterion of order, revealed by a hierarchical set of observables. This connection between harmonicity and order is effective for anharmonic systems undergoing a stochastic transition, but not for integrable systems, for example the Toda model. For these reasons, our experiments should be read with a different attitude than in the pure search for stochasticity, as a way to have an insight into the structure of the ordered domain. Actually, the fact that $\kappa_1, \ldots, \kappa_i$ are not only dependent on the initial conditions when $u < \tilde{u}_i$ but also *quasiharmonic* is an important feature *against* stochasticity; while the non-harmonic behaviour of $\kappa_{i+1}, \kappa_{i+2}, \ldots$ in itself does not imply anything about stochasticity.

Furthermore, in the previous section we insisted on two different features: (1) independence of N for $\tilde{u}_i$ at a fixed order i; (2) the vanishing of $\tilde{u}(N)$ as N grows. Of course, being based on extrapolations from actual simulations, these last features, the second one in particular, remain on a conjectural domain. Both aspects could be strictly related to the distinction between the so-called WST and SST respectively. Remember

that the SST has been defined through criteria accessible to numerical experiments (energy equipartition, Lyapunov exponents, independence from initial conditions etc), whereas the WST is not an experimental result: it is the supposed threshold from the quasi-integrable behaviour in the domain filled (in a measure theoretic sense) by the KAM tori. The Arnol'd diffusion, taking extremely long times, could indeed be responsible for transitivity on the energy surface, despite the existence of other conservation laws.

From the point of view of statistical mechanics, the relevant question is which of them is the 'true' stochasticity transition (TST), i.e. the transition (if any) from a behaviour non-compatible with standard statistics to an ordinary one. Experimentally, we see that the breakdown $\tilde{u}_1$ (or $\tilde{u}_\rho$) coincides with the SST. Moreover, at fixed N, the extrapolation at energies below $\tilde{u}(N)$ says that all curvatures attain the harmonic values. Then, we might conjecture that the WST has to do with $\tilde{u}(N)$, possibly that WST $= \tilde{u}(N)$. In any case this domain below $\tilde{u}(N)$ seems to rapidly shrink to 0 as N grows, exactly as the WST should do in the opinion of the weak chaos supporters. However, the request that *all* curvatures behave harmonically is extremely demanding, and it is more plausible that WST $> \tilde{u}(N)$.

What happens then in this intermediate region, where, at fixed energy density, a number of curvatures behave harmonically independently of N? In principle, such a domain could either deserve the denomination 'weakly stochastic' or 'weakly ordered'. A definite choice should solve in advance the problem of establishing which kind of ergodic measure holds there, and in particular if such a measure is continuous or not with respect to the Liouville measure. If the answer is yes, then the domain is weakly stochastic and TST $=$ WST; otherwise, it is weakly ordered and TST=SST. As far as we know, this problem is unsolved.

This last sentence seems to contrast the agreement, observed for example in [12], between dynamical and Monte Carlo simulations on geometrical observables based on Ricci and scalar curvatures. However, this agreement is achieved within standard experimental times, whereas, if it would depend on the weak chaos diffusion, averages below the SST should require longer and longer relaxation times. Therefore we are led to conclude that, more than to the weak chaos, the agreement is due to the intrinsic insensitivity of those observables to the initial conditions. Of course, this fact does not exclude their sensitivity, actually very high, to the SST. In the same sense, the crossover in the scaling law of the largest Lyapunov exponent does not exclude that at low energy the motion takes place on manifolds of reduced dimensionality [10, 11]. Even if our experiments do not face this problem directly (possible local disorder on such reduced manifolds), they stress the peculiarity of the SST, the robustness of quasiharmonicity and the (at least practical) difficulties in deriving the standard Liouville measure from dynamics.

More likely, the presence of harmonic constraints on the observables may be related to such phenomena as the 'superexponential stability' studied in [16], in the spirit of perturbation theory. In terms of a perturbation parameter given by the distance r from an invariant KAM torus, the speed of Arnol'd diffusion is evaluated indeed as $\exp[-\exp(1/r)]$. This seems beyond any possible numerical verification (see, however, [17] for the standard map), but our experiments up to the SST, i.e. in the non-purely perturbative domain, show the possibility that such estimates play a role even at the border of strong chaos.

References

[1] Alabiso C, Besagni N, Casartelli M and Marenzoni P 1996 *J. Phys. A: Math. Gen.* **29** 3733
[2] Benettin G, Galgani L and Strelcyn J M 1976 *Phys. Rev.* A **14** 2338
[3] Casartelli M and Sello S 1987 *Nuovo Cimento* B **97** 183
Casartelli M and Sello S 1985 *Phys. Lett.* **112A** 249

Casartelli M and Sello S 1987 *Advances in Nonlinear Dynamics and Stochastic Processes-II* ed G Paladin and A Vulpiani (Singapore: World Scientific)
[4] Pettini M and Landolfi M 1990 *Phys. Rev.* A **41** 768
[5] Pettini M and Cerruti-Sola M 1991 *Phys. Rev.* A **44** 975
[6] Alabiso C, Casartelli M and Marenzoni P 1993 *Phys. Lett.* A **183** 305
[7] Alabiso C, Casartelli M and Marenzoni P 1995 *J. Stat. Phys.* **79** 451
[8] Kantz H, Livi R and Ruffo S 1994 *J. Stat. Phys.* **76** 627
[9] Casetti L, Livi R and Pettini M 1995 *Phys. Rev. Lett.* **74** 375
[10] De Luca J, Lichtenberg A J and Lieberman M A 1995 *Chaos* **5** 283
[11] Poggi P and Ruffo S 1997 Exact solutions in the FPU oscillator chain *Preprint* Università di Firenze
[12] Pettini M 1993 *Phys. Rev.* E **47** 828
[13] Casetti L and Pettini M 1993 *Phys. Rev.* E **48** 4320
[14] Pettini M and Valdettaro R 1995 *Chaos* **5** 646
[15] Allendoerfer C B 1974 *Calculus of Several Variables and Differential Manifolds* (New York: Macmillan)
[16] Morbidelli A and Giorgilli A 1994 *J. Stat. Phys.* **78** 1607
[17] Lega E and Froeschlé C 1996 *Physica* **95D** 97